# Design of High-Efficiency and Low-Cost Six-Phase Permanent Magnet Synchronous Generator for Direct-Drive Small-Scale Wind Power Application

M. E. Moazzen*, S. A. Gholamian*(C.A.) and M. Jafari-Nokandi*

**Abstract:** Permanent magnet synchronous generators (PMSG) have a huge potential for direct-drive wind power applications. Therefore, optimal design of these generators is necessary to maximize their efficiency and to reduce their manufacturing cost and total volume. In this paper, an optimal design of a six-phase 3.5 KW direct-drive PMSG to generate electricity for domestic needs is performed. The aim of optimal design is to reduce the manufacturing cost, losses and total volume of PMSG. To find the best design, single/multi-objective design optimization is carried out. Cuckoo optimization algorithm (COA) is adopted to solve the optimization problem. Comparison between the results of the single-objective and multi-objective models shows that simultaneous optimization of manufacturing cost, losses and total volume leads to more suitable design for PMSG. Finally, finite-element method (FEM) is employed to validate the optimal design, which show a good agreement between the theoretical work and simulation results.

**Keywords:** Permanent Magnet Synchronous Generator (PMSG), Wind Power, Cuckoo Optimization Algorithm (COA), Finite Element Method (FEM).

## 1 Introduction

NOWADAYS, renewable energy is rapidly replacing other traditional sources of electricity generation like coal, gas and nuclear power. The contribution of wind energy in electricity generation, as one of the most important types of renewable energy sources, has grown swiftly over the past decade. In order to maximize the energy capture, minimize costs and improve power quality, various wind turbine concepts and wind generators have been developed [1]. High overall efficiency, high reliability and low maintenance are the major advantages of direct-drive wind turbine system compared to the geared drive [1], [2]. Focusing on the different types of generators, the permanent magnet (PM) generator has high potential for the direct-drive wind turbines compared to electrically excited generator, because of its lower failure rate, lack of slip rings and winding excitation, and consequently improvement of the efficiency [3], [4]. Therefore, several studies have concentrated their research on the PM wind generator, for example, an outer-rotor permanent magnet generator (PMG) for directly coupled

wind turbines has been studied in [5]. It is shown that a generator with a simple construction can operate with good and reliable performance over a wide range of wind speeds. In [6], forty-five direct-drive PM wind power generation systems with the different rated power levels and different rated rotational speeds have been optimally designed for the minimum generation system cost. Finally, the optimum results have been compared to each other. The optimal design and finite element analysis of a 2 MW direct drive permanent magnet wind generator has been proposed in [7]. The results indicate that to improve the EMF and reduce the flux leakage, the best pole-slot number and the optimal structure of pole shoe can be obtained by the comparison of different models. Eriksson and Bernhoff [8], have presented loss evaluation and optimal design for direct-drive wind power generator. Also, it is expressed that an optimized generator for a minimum of losses will have a high overload capability. In [9], the optimum design of permanent-magnet direct-drive generator, considering the cost uncertainty in raw materials, is developed with genetic algorithm. Potgieter and Kamper [10], have presented a cost-effective technique to reduce the cogging torque and improve the voltage quality in PM wind generators. A simple analytic optimization algorithm based on a well-known mathematical approach-Lagrange multiplier is used to maximize the apparent air-gap power transferred under tangential stress constraint for PM generator in [11]. In [12], a new surrogate-assisted multi-objective optimization algorithm is proposed to improve the power transmission and to reduce the noise, vibration and cost

* The authors are with the Department of Electrical and Computer Engineering of Babol Noshirvani University of Technology, P. O. Box 484, Babol, Iran.
E-mails: m.moazzen@stu.nit.ac.ir, gholamian@nit.ac.ir, m.jafari@nit.ac.ir.
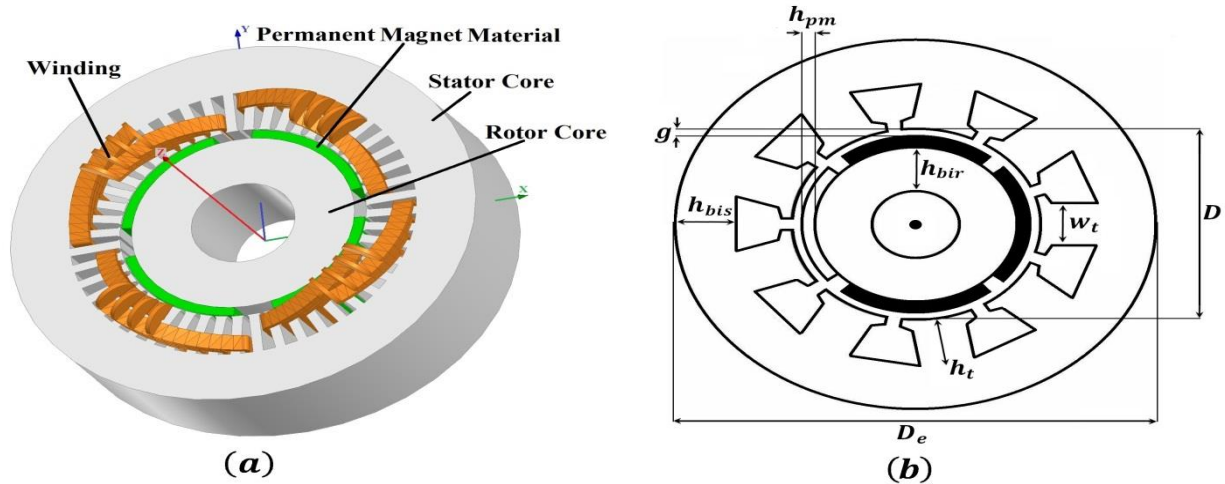Corresponding Author: S. A. Gholamian.

**Fig. 1** Configuration of a RS-PMG, schematic view (a), cross section (b).

of an interior permanent magnet synchronous motor for a fuel cell electric vehicle. In [13], a multi-component layout optimization method is proposed that incorporates parametric and topological design variables to determine the optimal permanent magnet shape of a permanent magnet actuator.

To increase the reliability of the ordinary three phase wind power system, six phase wind power system is proposed [14]. Beside their reliability, poly-phase electrical machines have many advantages compared to three phase machines, including lower total harmonic, reduced amplitude and increased frequency of pulsating torque and lower current per phase for the same rated voltage [15]. A direct-drive wind power generator has to operate at very low speeds. According to the electric machine design principles, these types of machine are characterized by the large dimensions and weight [5], [11]. The design of low-speed, large-dimension generators has to be optimized in terms of cost, total volume, and efficiency. In order to minimizing the generator losses, maximizing efficiency and improve the thermal characteristic of the generator, the generator losses is chosen as one of the objective functions. To reduce the total volume, weight and cost of generator and wind turbine structure, total volume and manufacturing cost of PMSG are chosen as other objective functions. Therefore, single/multi-objective optimizations have been done to find the best design for six-phase PMSG for direct-drive wind power. For this purpose, the equations needed for PMSG design are extracted and then the COA is used to optimal design.

The rest of this paper is organized as follows. The main equations needed for PMSG design are presented in Section 2. Generator losses are introduced in Section 3. In Section 4, cost estimation for PMSG manufacturing is presented. Wind turbine modeling and calculating shaft speed are presented in Section 5. In Section 6, cuckoo optimization algorithm is introduced. The design procedure is expressed in Section 7. Generator parameters and design variables are given in Section 8. In Section 9, optimal design is carried out. In

Section 10, the design validity is verified by 2-D finite element analysis. Finally, conclusions are given in Section 11.

## 2  Main Equations of PMSG Design

Different topologies of PM machines are possible to be used for direct-drive wind turbines but the radial-flux, surface-mounted permanent magnet generator (RS-PMG), due to simple structure and reliability, can be a good choice for this application [6]. Cross section and schematic view of RS-PMG are shown in Fig. 1. In this section, the main dimensions of RS-PMG are determined. Here, parallel-sided teeth are rectangular and stator slots are trapezoidal.

### 2.1  Main Dimensions

In order to establish an analytical relationship between the electromagnetic parameters and geometric dimensions of the machine, the air-gap apparent power is expressed as a function of the induced voltage and current on the armature (stator) winding as follows [16]:

$$S_g = mE_{ph}I_{ph} \tag{1}$$

where m is the number of phases. $E_{ph}$ is the rms value of fundamental no-load induced voltage in one phase of the stator winding and $I_{ph}$ is the rms current of the stator winding. $E_{ph}$ can be expressed as a function of the stator geometrical dimensions as follows [6]:

$$E_{ph} = \sqrt{2}k_{w1}N_{ph}\omega_m \frac{D}{2}LB_{mg1} \tag{2}$$

where $k_{w1}$ and $N_{ph}$ are the fundamental winding factor and the number of turns per phase, respectively. $\omega_m$ is the mechanical angular speed of the rotor. $D$ is the air-gap diameter (stator inner diameter). $L$ is the stator stack length. $B_{mg1}$ is the peak value of the first harmonic of the air gap magnetic flux density, which is [16]:

$$B_{mg1} = \frac{4}{\pi}B_{mg} \sin\left(\frac{\pi}{2}\alpha_i\right) \tag{3}$$

where $B_{mg}$ and $\alpha_i$ are the peak value of the air gap magnetic flux density and the pole-shoe arc to pole-pitch ratio, respectively. The range of values for $\alpha_i$ is selected between 0.6 and 0.9 in optimal design process [3]. $B_{mg1}$ and $B_{mg}$ are illustrated in Fig. 2. Meanwhile, for the sizing procedure of NdFeB PMSG can initially be estimated as $B_{mg} = (0.6 - 0.8) \times B_r$ , where $B_r$ is the residual flux density of PM [16]. The air gap apparent power of the generator as a function of main dimensions of machine can be given by:

$$S_g = 0.5\pi^2 k_{w1} n_s D^2 L A_m B_{mg1} \qquad (4)$$

where $n_s$ is rotational speed in rev/sec. $A_m$ is the peak value of the stator linear current density, which can be expressed as [16]:

$$A_m = \frac{2m\sqrt{2}N_{ph}I_{ph}}{\pi D} \qquad (5)$$

Finally, the main dimensions of the generator as a function of output power can be given by:

$$D^2 L = \frac{P_{out}\varepsilon}{n_s \sigma_p} \qquad (6)$$

$$\sigma_p = 0.5\pi^2 k_{w1} A_m B_{mg1} \cos\varphi \qquad (7)$$

where $P_{out}$ is the output power of the generator. $\varepsilon$ is the no-load to rated load terminal phase voltage ratio. $\sigma_p$ is the output coefficient. $\cos\varphi$ is the load power factor. The direct-drive PMSG connected to the grid via back-to-back converter, which is also characterized by almost unity power factor [17]. The relative apportionment of the air-gap diameter and stator stack length in electrical machine design depends on the machine application. The suitable range of values for ratio $L/D$ is typically 0.14 - 0.5 for direct-drive PM wind generator applications [18].

## 2.2 Magnet Dimensions

The magnet thickness to provide the excitation required on the air gap can be expressed as [2]:

$$h_{pm} = \frac{B_{mg}\mu_{rec} g_{eff}}{B_r} \qquad (8)$$

where $\mu_{rec}$ is the relative permeability of the PM materials. $g_{eff}$ is the effective air gap, which can be calculated as [2]:

$$g_{eff} = k_c \left( g + \frac{h_{pm}}{\mu_{rec}} \right) \qquad (9)$$

where $k_c$ and $g$ are the Carter's coefficient and mechanical air-gap diameter, respectively.
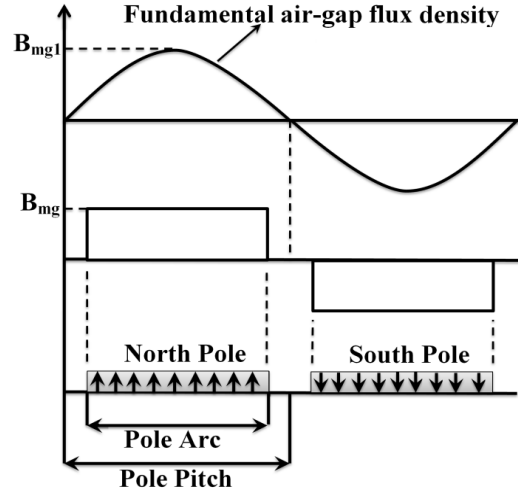


**Fig. 2** The air-gap magnetic flux distribution ideal curve in one pole pitch.

## 3 Generator Losses

The losses considered in this paper are the stator iron losses, the copper losses, ventilation and windage losses and additional losses. The stator iron losses can be divided into hysteresis losses and eddy current losses. The rotor iron losses are neglected.

## 3.1 Core Losses

The stator core losses in the separate parts, i.e., teeth and back iron, are estimated by determining the peak flux density in the teeth and back iron. Therefore, the core losses in the back iron or teeth of the stator can be calculated as [3]:

$$\begin{aligned} P_{Fe} &= k_h m_{fe} \rho_h \frac{f}{f_{base}} \left( \frac{B_{Fe}}{B_{base}} \right)^2 \\ &+ k_e m_{fe} \rho_e \left( \frac{f}{f_{base}} \right)^2 \left( \frac{B_{Fe}}{B_{base}} \right)^2 \end{aligned} \qquad (10)$$

where f is the rated frequency of the generator. $k_h$ and $k_e$ are the empirical factors for the hysteresis and eddy current losses, respectively. $m_{fe}$ is the weight of the core in the back iron or teeth of the stator. $\rho_h$ and $\rho_e$, respectively are the specific hysteresis losses and the specific eddy current losses in W/kg at frequency $f_{base}$ and flux density $B_{base}$. $B_{Fe}$ is the maximum flux density in the back iron or tooth of the stator. The core used for the stator is Surahammar CK-30 [3]. Values of $k_h$, $k_e$, $\rho_h$, $\rho_e$ and $B_{Fe}$ are given in Table 1.

## 3.2 Copper Losses

The copper losses can be calculated as:

$$P_{cu} = m R_s I_{ph}^2 \qquad (11)$$

where $R_s$ is the stator winding resistance per phase,

which can be expressed as:

$$R_s = \frac{\rho_{cu} L_t N_{ph}}{a_s} \qquad (12)$$

where $\rho_{cu}$ is the copper resistivity ($\frac{1}{57} \times 10^{-6}$ at 20°C) [16]. $N_{ph}$ and $a_s$ are the number of turns per phase and the conductor cross section, respectively. $L_t$ is the average length of the one turn per phase, which can be calculated as:

$$L_t = 2(L + L_{ew}) \qquad (13)$$

where $L_{ew}$ is the end-winding length, which referring to Fig. 3, can be approximated as [19]:

$$L_{ew} = \frac{\Pi}{2} \frac{y'_s + w_t}{2} + y'_s K_{ov}(y - 1) \qquad (14)$$

where $y'_s$, is the slot pitch measured at the half height of the stator tooth, which can be calculated by Eq. (15). $y$ is the coil pitch (in number of slots). $K_{ov}$ is the increasing factor. This factor is considered due to the end-winding overlapping. The range of values for $K_{ov}$ is 1.6-2 [19].

$$y'_s = \frac{\pi(D + h_t)}{Q} \qquad (15)$$

where $Q$ and $h_t$ are the number of slots and stator tooth height, respectively.

### 3.3 Windage and Ventilation Losses

The windage and ventilation losses can be calculated as [20]:

$$P_\rho = K_{rb} D_r (L + 0.6\tau_P) \left(2\pi n_r \frac{D_r}{2}\right)^2 \qquad (16)$$

where $K_{rb}$ is an empirical factor, which depends on the cooling system. $D_r$, $\tau_P$ and $n_r$ are the rotor diameter, the pole pitch and the rotational shaft speed in rev/sec, respectively.

### 3.4 Additional Losses

The additional losses are very difficult to calculate and are commonly determined as a fraction of the output power as follows [20]:

$$P_{str} = k_{str} P_{out} \qquad (17)$$

The range of values for $k_{str}$ is 0.0005–0.0015 for Nonsalient-pole synchronous machine [20]. Considering different components of generator losses, the total power losses Ploss is:

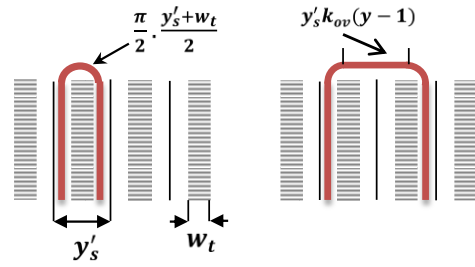$$P_{loss} = P_{cu} + P_{Fe} + P_\rho + P_{str} \qquad (18)$$



**Fig. 3** End-winding calculation.

### 4 Cost Estimation of PMSG Manufacturing

PMSG manufacturing cost can (U.S. dollars) be expressed as [16]:

$$C_t = k_N (C_w + C_c + C_{PM} + C_{Sh}) \qquad (19)$$

where $k_N$ is the coefficient depending on the number of manufactured generators per annum. In this paper, $k_N$=1 is assumed. $C_w$, $C_c$, $C_{PM}$ and $C_{Sh}$ are the cost of winding, core, PMs and shaft, respectively.

### 5 Wind Turbine Model and Shaft Speed

A wind turbine converts the wind kinetic energy into electrical energy. The available rated shaft power in three-bladed horizontal axial wind turbines can be calculated as a function of the rated wind speed as [2]:

$$P_t = \frac{1}{2} C_p \rho_{air} \pi R^2 u^3 \qquad (20)$$

where $C_p$ is the conversion efficiency with typical values between 0.3 and 0.45 [21]. $\rho_{air}$ is the air density which is 1.2 kg/m3 [21]. $R$ is the radius of the turbine blade. $u$ is the rated wind speed. The rated shaft speed (rad/s) of the RS-PMG can be estimated as [6], [21]:

$$\omega_r = \sqrt{\frac{0.5\rho_{air} \pi \lambda^2 u^5 C_p \eta}{P_{out}}} \qquad (21)$$

where $\eta$ is the generator efficiency, which is assumed 0.9 [6]. $\lambda$ is the tip speed ratio, which its range of values is 6–8 [6] or 5–7 [21]. The wind speed is an important parameter for calculating the nominal shaft speed. Investigations show that the range of wind speed, in the Nehbandan-zabol road of Iran, is 5-10.2 m/s [22]. Therefore, our generator is designed for operation at the wind speed of 10.2 m/s. According to nominal wind speed, the shaft speed is determined to be 250 rpm or 4.167 rev/s. For small-scale PM wind generators, the normal frequency range is reported as 30-80 Hz [5] or 10-70 Hz [18]. Therefore, considering the nominal frequency of generator as 12.5 Hz, the required number of poles to produce electricity in normal frequency range and nominal shaft speed referring to Eq. (22) is chosen as 6.

$$p = \frac{2f}{n_s} \qquad (22)$$

## 6 Cuckoo Optimization Algorithm

One of the recently developed meta-heuristic optimization algorithms is the cuckoo optimization algorithm (COA) which is an efficient approach to solve engineering optimization problems. In Comparison to standard versions of Particle Swarm Optimization (PSO) and Genetic Algorithm (GA), COA has converged faster in less iterations. The COA is inspired by the life of a bird family, called Cuckoo. Mother cuckoos never build their own nests and lay eggs in the nest of other birds. These eggs grow and become a mother cuckoo, if they are not recognized and not killed by host birds. In order to maximize their eggs survival rate, Cuckoos search for the most suitable area to lay eggs. Therefore, groups of cuckoos migrate to find the best environment for reproduction. The best environment for reproduction is the best result of objective functions [23].

## 7 Design Procedure

The design procedure is illustrated as a flowchart in Fig. 4.

## 8 Generator Parameters and Design Variables

Here, the optimal design of a 3.5 kW RS-PMG for wind turbines applications is presented. This generator has symmetrical 60o displacement windings. Six stator phases are divided into two Y-connected three-phase sets, labeled ABC and XYZ. The main design parameters of generator are expressed in Table 1. Design variables and their variation boundaries are given in Table 2. Neodymium iron boron magnet with the grade of NdFe35 is selected as PM material.

## 9 Optimal Design Results

In order to evaluate different design objectives, four different optimization models are conducted in this
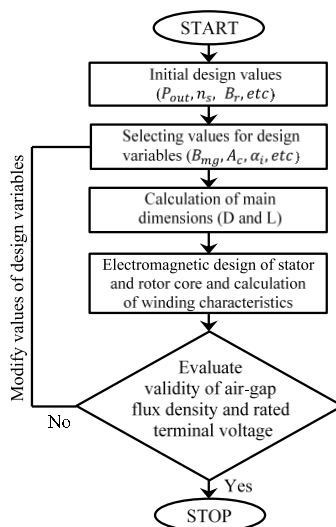


**Fig. 4** Design flowchart of the RS-PMG.

**Table 1** Modeling constants and main design parameters of generator.

| Parameters and Constants | Value |
|---|---|
| **Main Design Parameters** | |
| Rated output power [w] | 3500 |
| Rated phase voltage ($V_{ph}$) [V] | 250 |
| Rated shaft speed [rpm] | 250 |
| Rated frequency [HZ] | 12.5 |
| Number of poles | 6 |
| Number of distributed short-pitch winding layers | 2 |
| Air-gap diameter ($g$) [mm] | 0.5 |
| Current density [A/mm$^2$] | 5 |
| Number of slots per pole and phase | 3 |
| Residual PM flux density [T] | 1.23 |
| Stator and Rotor yoke maximum flux density [T] | 1.5 |
| Stator tooth maximum flux density [T] | 1.6 |
| | |
| **Loss Modeling Constants** | |
| $f_{Base}$ [HZ] | 50 |
| $B_{Base}$ [T] | 1.5 |
| $k_h$ for stator back iron | 2 |
| $k_e$ for stator back iron | 1.8 |
| $k_h$ for stator teeth | 1.2 |
| $k_e$ for stator teeth | 2.5 |
| $k_{ov}$ | 1.8 |
| $K_{rb}$ | 10 |
| $k_{str}$ | 0.0015 |
| $\rho_h$ [W/kg] | 2.04 |
| $\rho_e$ [W/kg] | 0.76 |
| | |
| **Wind Turbine Modeling Constants** | |
| $C_p$ | 0.3 |
| $\lambda$ | 6.5 |

**Table 2** Design variables and their variation boundaries.

| Design variables | Boundary |
|---|---|
| $B_{mg}$ [T] | 0.738 – 0.984 |
| $A_m$ [A/m] | 10000 - 55000 |
| $\alpha_i$ | 0.6 – 0.9 |
| $\epsilon$ | 1.05 – 1.4 |
| $L/D$ | 0.14 – 0.5 |

study which can briefly be described as follows:
**Case1:** in this case, the objective is minimizing generator losses, which can be represented as:

$$Min\ F_1 = P_{loss} \tag{23}$$

**Case 2:** in this case, the objective is minimizing manufacturing cost of the generator, which can be expressed as:

$$Min\ F_2 = C_t \tag{24}$$

**Case 3:** in this case, the objective is minimizing total volume of the generator, which can be expressed as

$$Min\ F_3 = \left(\frac{D_e}{2}\right)^2 .\pi.L \tag{25}$$

**Case 4:** in this case, the objective is minimizing

**Table 3** The optimization results.

| Parameter | Minimum Losses Design (F₁) | Minimum Cost Design (F₂) | Minimum Volume Design (F₃) | Multi Objective Design (F₄) |
|---|---|---|---|---|
| Losses [w] | 243.10 | 333.39 | 329.50 | 322.98 |
| Cost [$] | 1075.19 | 499.66 | 503.83 | 507.78 |
| Volume [Cm³] | 17041.12 | 7697.47 | 7615.99 | 7666.46 |
| Efficiency (%) | 93.5 | 91.30 | 91.39 | 91.55 |
| **Optimal Design Variables** | | | | |
| $A_m$ [A/m] | 15508.58 | 55000 | 55000 | 54576.21 |
| $B_{mg}$ [T] | 0.983 | 0.984 | 0.984 | 0.984 |
| $\alpha_i$ | 0.8352 | 0.8028 | 0.8715 | 0.8752 |
| $L/D$ | 0.4783 | 0.4726 | 0.4069 | 0.4970 |
| $\epsilon$ | 1.05 | 1.1753 | 1.1779 | 1.1528 |

**Table 4** The comparison between cases with minimum values of losses, cost and volume.

| | Cases | | | |
|---|---|---|---|---|
| | Case 1 | Case 2 | Case 3 | Case 4 |
| Minimum Power Losses (243.10 W) | 0 | 37.14% | 35.54% | 32.85% |
| Minimum Cost (499.66 $) | 115.18% | 0 | 0.83% | 1.62% |
| Minimum Volume (7615.99 Cm³) | 123.75% | 1.06% | 0 | 0.66% |
| Average Deviations | 79.64% | 12.73% | 12.12% | 11.71% |

generator losses, manufacturing cost and total volume, simultaneously. To this end, flexible objective function is defined as:

$$Min\ F_4 = \frac{1}{\alpha}F_1 + \frac{1}{\beta}F_2 + \frac{1}{\gamma}F_3 \qquad (26)$$

where $\alpha$, $\beta$, $\gamma$ are the minimum values of the $F_1$, $F_2$ and $F_3$, respectively. Fig. 5 plots the $F_4$ minimization for the first 50 iterations. Results are shown in Table 3. It can be observed that any attempt to achieve a single objective optimal design, deteriorate other characteristics. Therefore, multi-objective optimization would be necessary to make a satisfactory compromise among performance indices or objectives. Referring to Table 4, the comparison between cases with minimum values of generator losses, total volume and

manufacturing cost shows that the simultaneous optimization of the generator with minimum average deviations (11.71%) leads to suitable design for PM wind generator.

## 10 Finite Element Analysis

In order to verify the analytical design procedure presented in the previous sections, simulation results are obtained using the FEM and are compared with those of the analytical model. Characteristics and dimensions of the optimized RS-PMG are given in Table 5. The B-H curve of the stator and rotor laminated core is presented



**Fig. 5** The value of $F_4$ at each iteration for the first 50 iterations.

**Table 5** Optimal generator parameters.

| Parameter | Value | Unit |
|---|---|---|
| Stator outer diameter ($D_e$) | 321.4 | mm |
| Stator inner diameter ($D$) | 190.1 | mm |
| Stator stack length ($L$) | 94.5 | mm |
| Stator yoke thickness ($h_{bis}$) | 29.5 | mm |
| Rotor yoke thickness ($h_{bir}$) | 29.5 | mm |
| Stator tooth width ($w_t$) | 3.5 | mm |
| Stator tooth height ($h_t$) | 36.2 | mm |
| Stator slot width ($w_s$) | 4.14 | mm |
| Magnet thickness ($h_{pm}$) | 3.3 | mm |
| Number of turns per phase ($N_{ph}$) | 828 | - |
| Number of conductors per slot | 92 | - |
| Number of parallel branches of winding | 1 | - |
| Coil pitch | 12 | - |
| Maximum air-gap flux density ($B_{mg}$) | 0.984 | T |
| RMS fundamental induced voltage ($E_{ph}$) | 289.94 | V |
| Stator yoke maximum flux density ($B_{bis}$) | 1.5 | T |
| Rotor yoke maximum flux density ($B_{bir}$) | 1.5 | T |
| Stator tooth maximum flux density ($B_{ts}$) | 1.6 | T |

in the Appendix A. The Ansoft-MAXWELL v.16 software, which is a FEM based software, is used for simulation. The magnetic flux density and flux lines distribution of the optimized generator due to the PM materials is depicted in Fig. 6. The mesh diagram of the generator finite element model is shown in Fig. 7.

The waveform of six-phase terminal voltage at rated load is presented in Fig. 8 with the rms value of 248.82 (V). The total harmonic distortion (THD) of terminal phase voltage is measured 0.96%. Table 6 compares the results of the analytical optimization with those of the finite-element analysis. Obviously, there is a good agreement between the optimal design results and the finite-element analysis.

## 10  Conclusion

In this paper, cuckoo optimization algorithm is employed to solve the single/multi-objective design of a six-phase 3.5 KW direct-drive PMSG considering total volume, manufacturing cost and generator losses as
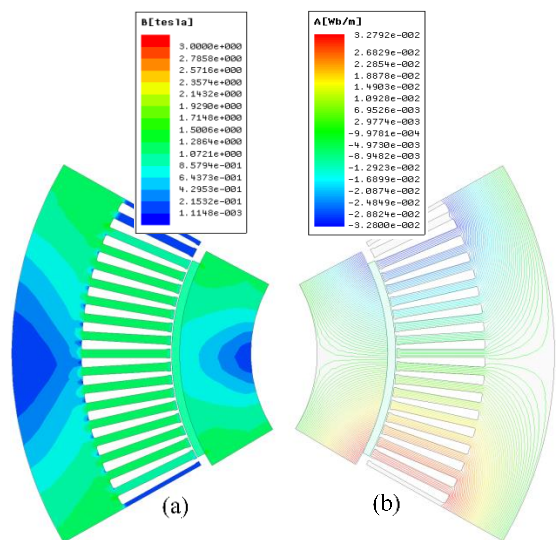


**Fig. 6** Magnetic flux density distribution (a), flux lines distribution of the optimized RS-PMG (b).
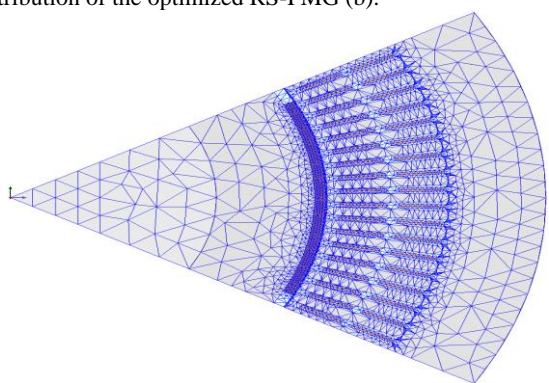


**Fig. 7** The finite element mesh of the generator.
three objectives. For this purpose, the main equations of

generator design are extracted. It was shown that simultaneous optimization of the generator losses, manufacturing cost and total volume with minimum average deviations leads to more suitable design for generator. Two-dimensional finite element analysis results verify the results of the proposed optimal design.
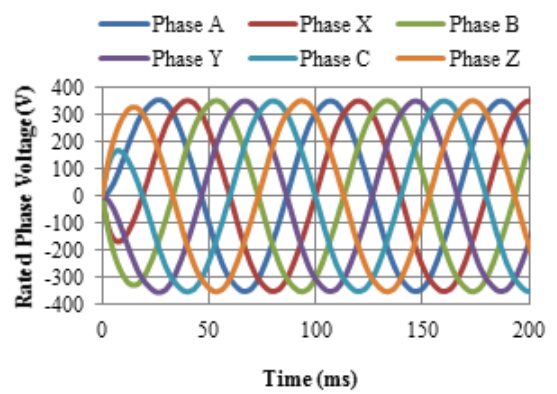


**Fig. 8** The waveform of six-phase terminal phase voltage at rated load.

**Table 6** Comparison of analytical optimization and FEM results.

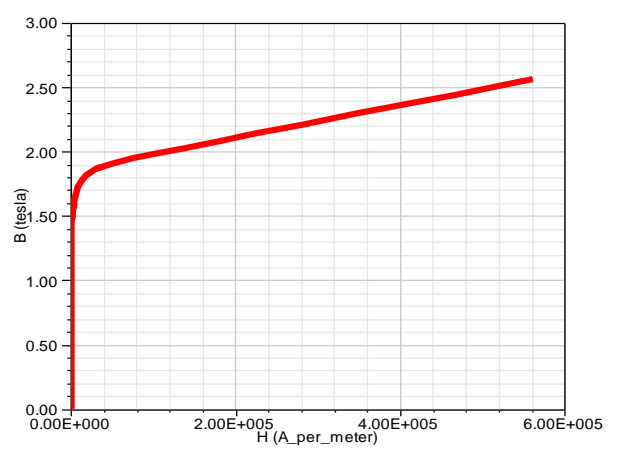| Generator Parameters | Analytical Model | FEM | Error (%) |
|---|---|---|---|
| $B_{mg}$ [T] | 0.984 | 0.9833 | 0.071 |
| $E_{ph}$ [V] | 289.94 | 284.52 | 1.86 |
| $V_{ph}$ [V] | 250 | 248.82 | 0.47 |
| $B_{bis}$ [T] | 1.5 | 1.42 | 5.33 |
| $B_{bir}$ [T] | 1.5 | 1.49 | 0.67 |
| $B_{ts}$ [T] | 1.6 | 1.58 | 1.25 |

## Appendix A



**Fig. A1** The B-H curve of the laminated core.

## References

[1] T. Gundogdu and G. Komurgoz, "Technological and Economical Analysis of Salient Pole and Permanent Magnet Synchronous Machines Designed for Wind Turbines," *J. Magn. Magn. Mat.*, vol. 324, no. 17, pp. 2679–2686, Aug. 2012.

[2] H. Li et al., "Optimization of Multibrid Permanent-Magnet Wind Generator Systems," *IEEE Trans. Energy Convers.*, vol. 24, no. 1, pp. 82-92, Mar. 2009.

[3] A. Grauers, "Design of direct-driven permanent-magnet generators for wind turbines," *Ph.D. dissertation*, Chalmers Univ. Technol., Goteborg, Sweden, 1996.

[4] H. Polinder et al., "Comparison of direct-drive and geared generator concepts for wind turbines," *IEEE Trans. Energy Convers.*, vol. 21, no. 3, pp. 725-733, Sept. 2006.

[5] J. Chen et al., "Design and Finite-Element Analysis of an Outer-Rotor Permanent-Magnet Generator for Directly Coupled Wind Turbines," *IEEE Trans. Magn.*, vol. 36, no. 5, pp. 3802-3809, Sept. 2000.

[6] H. Li and Z. Chen, "Design Optimization and Site Matching of Direct-Drive Permanent Magnet Wind Power Generator Systems," *J. Renew. Energy*, vol. 34, no. 4, pp. 1175–1184, Apr. 2009.

[7] G. Duan et al., "Direct Drive Permanent Magnet Wind Generator Design and Electromagnetic Field Finite Element Analysis," *IEEE Trans. Appl. Supercond.*, vol. 20, no. 3, pp. 1883-1887, Jun. 2010.

[8] S. Eriksson and B. Bernhoff, "Loss Evaluation and Design Optimization for Direct Driven Permanent Magnet Synchronous Generators for Wind Power," *J. Applied Energy*, vol. 88, no. 1, pp. 265–271, Jan. 2011.

[9] M. Pinilla and S. Martinez, "Optimal Design of Permanent-Magnet Direct-Drive Generator for Wind Energy Considering the Cost Uncertainty in Raw Materials," *J. Applied Energy*, vol. 41, pp. 267–276, May 2012.

[10] J. H. J. Potgieter and M. J. Kamper, "Torque and Voltage Quality in Design Optimization of Low-Cost Non-Overlap Single Layer Winding Permanent Magnet Wind Generator," *IEEE Trans. Ind. Electron.*, vol. 59, no. 5, pp. 2147-2156, May 2012.

[11] J. A. Tapia et al., "Optimal Design of Large Permanent Magnet Synchronous Generators," *IEEE Trans. Magn.*, vol. 49, no. 1, pp. 642-650, Jan. 2013.

[12] D. K. Lim et al., "Optimal Design of an Interior Permanent Magnet Synchronous Motor by Using a New Surrogate-Assisted Multi-Objective Optimization," *IEEE Trans. Magn.*, vol. 51, no. 11, pp. 7504-7507, Jan. 2015.

[13] S. Lim et al., "Multi-Component Layout Optimization Method for the Design of a Permanent Magnet Actuator," *IEEE Trans. Magn.*, vol. 52, no. 3, pp. 5304-5307, Mar. 2016.

[14] G. K. Singh, "Modeling and Analysis of Six-Phase Synchronous Generator for Stand-Alone Renewable Energy Generation," *J. Energy*, vol. 36, no.9, pp. 5621–5631, Sep. 2011.

[15] L. Parsa, "On Advantages of Multi-Phase Machines," in *31th Annu. IEEE Ind. Electron. Conf.*, Raleigh, NC, USA, 2005, pp. 1-6.

[16] J. F. Gieras, *Permanent Magnet Motor Technology: Design and Applications*, 3rd ed. New York, CRC Press, 2010.

[17] I. Boldea, *Variable speed generators*, 1st ed., New York, CRC Press, 2005.

[18] A. Khan and P. Pillay, "Design of a PM Wind, Optimized for Energy Capture over a Wide Operating Range," in *2005 IEEE Int. Elect. Mach. Drives Conf.*, San Antonio, TX, USA, 2005, pp. 1501-1506.

[19] N. Bianchi et al., "Design Criteria for High-Efficiency SPM Synchronous Motors," *IEEE Trans. Energy Convers.*, vol. 21, no. 2, pp. 396-404, Jun. 2006.

[20] J. Pyrhonen et al., "Heat Transfer," in *Design of Rotating Electrical Machine*,1st ed. Chichester, UK: Wiley, 2009, pp. 477-479.

[21] H. Jagau et al., "Design of a Sustainable Wind Generator System Using Redundant Material," *IEEE Trans. Ind. Appl.*, vol. 23, no. 6, pp. 1827-1837, Nov. 2012.

[22] Renewable Energy Organization of Iran. (2010). *Iranian Renewable Energy Organization Magazine* [Online]. Available: http://www.satba.gov.ir/suna_content/media/image/2015/11/4222_orig.pdf

[23] R. Rajabioun, "Cuckoo Optimization Algorithm," *J. Soft Comput.*, vol. 11, no. 8, pp. 5508–5518, Dec. 2011.

**Mohammad Ebrahim Moazzen** was born in Mazandaran, Iran, in 1989. He received the M.Sc degree in electrical engineering from Babol Noshirvani University of Technology, Babol, Iran in 2014. His special fields of interest include electric machine design.

**Sayyed Asghar Gholamian** was born in Mazandaran, Iran. He received the PhD degree in electrical engineering from K.N. Toosi University of Technology, Tehran, Iran in 2008. He is currently an assistant professor in the department of Electrical Engineering at the Babol

University Noshirvani of Technology, Babol, Iran. His research interests include design, simulation, modeling and control of electrical machines.

**Meysam Jafari-Nokandi** received the B.Sc degree from Sharif University of Technology, Tehran, Iran, in 2003 and the M.Sc and Ph.D degree from University of Tehran, Tehran, Iran, in 2005 and 2011, respectively, both in electrical engineering. He has joined faculty of Electrical and Computer Engineering, Babol Noshirvani University of Technology since 2011.His research interests are power market and power system reliability, operation and planning.